JOURNAL OF ALGEBRAIC STATISTICS
Volume 13, No. 2, 2022, p. 2619 - 2631
https://publishoa.com
ISSN: 1309-3452

Impact of chemical reaction towards MHD heat and mass transfer of a Jeffrey fluid flow with viscous dissipation and joule heating over a porous stretching sheet

B. Reddappa[1*], M. Sudheer Babu[1], K. A. Ajmath[1], M. Ravichand[1]
[1] Department of BS&H, Sree Vidyanikethan Engineering College, Tirupati-517102, A. P., India
**Corresponding author: drbreddappa@gmail.com*

ABSTRACT

In the presence of an external magnetic field, a study of the effects of chemical reactions on heat and mass transfer in a Jeffrey fluid flow through a porous stretched sheet is done. Similarity variables may be used to translate the controlling nonlinear partial differential equations into nonlinear ordinary differential equations. The MATLAB BVP4c technique is used to generate numerical results. In a graphic representation, the impacts of different restrictions on flow velocity, temperature, and concentration are indicated. There are thus studies done on the friction factor, Nusselt and Sherwood numbers, radiation, and internal heat production or absorption based on various values of the Jeffrey, response rate, and magnetic fields as well as other system factors like as suction and porosity. The study's conclusions are widely accepted in the scientific community today.

Keywords: Chemical reaction; MHD; joule heating; Stretching sheet; Jeffrey fluid; Porous medium.

1. Introduction

Non-Newtonian fluid flow modelling and understanding are essential for industrial and engineering applications because they are both basic and practical. Radiation-sensitive fluids, such as heavy oils and greases, paper coating, plasma and mercury sulphide, need a knowledge of the fluid's rheological characteristics to be used effectively. The shear tension and shear rate are not linearly related in these fluids. Non-Newtonian fluids' equations are much more complicated and higher-order than those of viscous fluids. Differential, rate, and integral fluids may be used to classify non-Newtonian fluids. Non-Newtonian fluids fall under the rate type group. This analysis takes into consideration the Jeffrey fluid model. In this fluid model, the relaxation to retardation time ratio and the retardation time may be seen. Studies by Kothandapani and Srinivas [1], Tripathi et al. [2], Hayat et al. [3], Abbasi et al. [4] and Farooq et al. [5] all cite the Jeffrey fluid model. MHD free convection flow of Casson fluid across a porous medium was explored by Sudheer Babu et al. in connection to second-order chemical processes and double stratification [6].

Magnetic hydrodynamic flow and heat transfer have been studied by several researchers, including Abo-Eldhab [7] and Chakarbati et al. [8]. Researchers are increasingly interested in porous sheets as technical applications such as flow through packed beds, pollution of the environment, and blood theology continue to rise in prominence. Varjravelu et al. [9] examined the laminar flow and heat transfer of a viscous fluid on a stretched surface with viscous dissipation. Chamkha [10] studied the influence of thermal radiation on MHD forced convection laminar flow in the presence of a heat source or sink. Using a vertical plate with a power-law variation in surface temperature, Abo-Eldahab [11] and colleagues investigated magnetic hydrodynamic free convection in the presence of Hall and ion-slip currents. Transient magneto hydrodynamic mixed double diffusive convection over a vertical plate submerged in non-Darcy porous material was studied by Jaber [12] using either suction or injection. Magnetic and Hall currents were employed to examine heat and mass transfer over a vertical plate in Abo-Eldahab and Elbarbary's work [13]. It was found that Hall current and Joule heating were both present when an electrically conducting fluid passed across a semi-infinite plate in a strong magnetic field with heat generation and absorption [14]. Magnetic hydrodynamic flow in the presence of radiation was studied by Jaber [15] using a continually growing vertical plate. Hall

JOURNAL OF ALGEBRAIC STATISTICS
Volume 13, No. 2, 2022, p. 2619 - 2631
https://publishoa.com
ISSN: 1309-3452

currents and fluid properties were examined. Many systems subjected to large changes in gravitational force or working at high speeds rely heavily on natural convection because of the influence of viscous dissipation. Jaber [16] investigated the magneto hydrodynamic flow of a fluid with variable properties over a stretched vertical plate. [17] MHD couette flow between thick arbitrarily conducting plates in a rotating configuration was studied by Mandal and coworkers. The heat flux, or thermal flux, is the rate at which heat energy is transmitted over a given surface in a given period of time. Mandal and colleagues [18] investigate an exponentially expanding porous sheet submerged in a porous liquid with varying surface heat flux. [19] Reddappa & Sreenadh investigated the effect of double stratification on electrical MHD free convection Jeffrey flow through an exponentially growing sheet. Reddappa et al. investigated the boundary layer flow of a thermally conducting Jeffrey fluid across a stratified exponentially extending sheet [20]. Nagur Meeraiah et al. [21] have discussed in detail the Casson fluid flow and heat transfer via a stretched sheet with unsteady MHD boundary layer flow.
Chemical reactions and their impact on MHD heat and mass transfer in a Jeffrey fluid flow with viscosity depletion and joule heating are being studied in this field. An ordinary differential system may be converted to an ordinary differential system by using similarity variables. Bvp4c is used to quantitatively solve the following relations. For each fluid parameter, the non-dimensional values are shown visually. Tables show the differences between this article and the existing body of literature.

2. Formulation of the Problem

Jeffrey fluid flow is used to heat a viscous sheet using Ohmic dissipation (joule heating) and heat generation/absorption effects in an exponentially growing sheet. Normally, the sheet is exposed to a high-intensity magnetic field that is maintained throughout time. The induced magnetic field is disregarded if the Reynolds number of the magnet is assumed to be low. For example, let's say that the surface is stretched at the velocity $U = U_0 e^{x/L}$, where U_0 and L is the reference speed and length, respectively. This is the underlying premise. The flow geometry may be seen in Figure 1. Increasing or decreasing the pace is a choice. On the sheet, a constant flow of heat q_w and fluid temperature T_∞ are maintained.

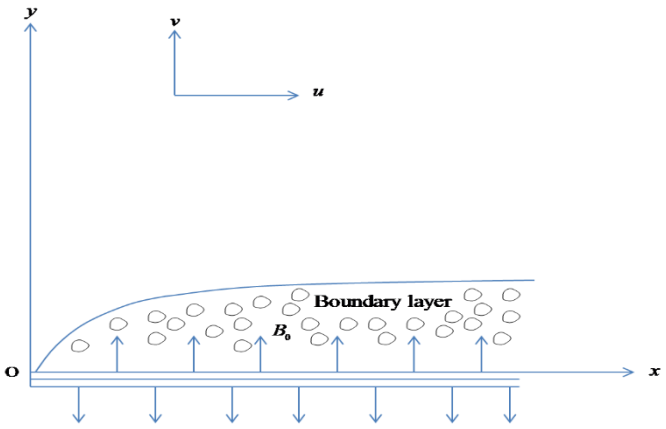

Fig. 1. Coordinate system and physical model.

Under these conditions, the governing equations take the following form:

JOURNAL OF ALGEBRAIC STATISTICS
Volume 13, No. 2, 2022, p. 2619 - 2631
https://publishoa.com
ISSN: 1309-3452

$$\frac{\partial u}{\partial x}+\frac{\partial v}{\partial y}=0 \tag{1}$$

$$u\frac{\partial u}{\partial x}+v\frac{\partial u}{\partial y}=\frac{\mu}{\rho\left(1+\lambda_1\right)}\frac{\partial^2 u}{\partial y^2}-\frac{\sigma B_0^2 u}{\rho}-\frac{\upsilon u}{K_p^*} \tag{2}$$

$$u\frac{\partial T}{\partial x}+v\frac{\partial T}{\partial y}=\frac{k}{\rho C_p}\frac{\partial^2 T}{\partial y^2}-\frac{1}{\rho C_p}\frac{\partial q_r}{\partial y}+\frac{q'''}{\rho C_p}\left(\frac{\partial u}{\partial y}\right)^2+\frac{\sigma B_0^2 u^2}{\rho C_p} \tag{3}$$

$$u\frac{\partial C}{\partial x}+v\frac{\partial C}{\partial y}=D\frac{\partial^2 C}{\partial y^2}-K_1\left(C-C_\infty\right) \tag{4}$$

The boundary conditions are

$$u=U,\ v=-v_w,\ -k\left(\frac{\partial T}{\partial y}\right)=q_w,\ -k\left(\frac{\partial C}{\partial y}\right)=q_w \ \text{ at } \ y=0 \tag{5}$$

$$u\to 0,\ T\to T_\infty,\ C\to C_\infty \text{ as } y\to\infty \tag{6}$$

Here, it is assumed that $v_w=v_0e^{x/2L}$, where v_0 is a constant.

Hossain et al. [22] and Raptis [23] among others use the Rosseland diffusion approximation to estimate the radiative heat flow

$$q_r=-\frac{4\sigma^*}{3k^*}\frac{\partial T^4}{\partial y} \tag{7}$$

Where σ^* and k^* are the Stefan-Boltzmann constant and the mean absorption coefficient, respectively. We presume that the temperature difference within the flow adequately small. The expression T^4, enlarging in a Taylor series in powers of $\left(T-T_\infty\right)$ and neglecting higher-order terms we get

$$T^4\approx 4T_\infty^3T-3T_\infty^4$$

Hence, $q_r=-\dfrac{16\sigma^*T_\infty^3}{3k^*}\dfrac{\partial T}{\partial y}$

then $\dfrac{\partial q_r}{\partial y}=-\dfrac{16\sigma^*T_\infty^3}{3\rho C_pk^*}\dfrac{\partial^2 T}{\partial y^2}$ (8)

The stream function $\psi\left(x,y\right)$ defined by

$$u=\frac{\partial\psi}{\partial y},\ v=-\frac{\partial\psi}{\partial x} \tag{9}$$

Which satisfies the equation of continuity (1).

JOURNAL OF ALGEBRAIC STATISTICS
Volume 13, No. 2, 2022, p. 2619 - 2631
https://publishoa.com
ISSN: 1309-3452

Introducing the similarity transformation:

$$\eta = y\sqrt{\frac{U}{2\upsilon L}},\ u = Uf'(\eta),\ v = -\sqrt{\frac{\upsilon U}{2L}}\left(f(\eta)+\eta f'(\eta)\right),\ \theta(\eta) = \frac{k}{q_w}(T-T_\infty)\sqrt{\frac{\mathrm{Re}}{2L^2}},$$

$$\phi(\eta) = \frac{k}{q_w}(C-C_\infty)\sqrt{\frac{\mathrm{Re}}{2L^2}},\ M = \frac{2\sigma B_0^2 L}{\rho U},\ \mathrm{Pr} = \frac{\mu C_p}{k},\ R = \frac{16\sigma^* T_\infty^3}{3k^* k},\ f_w = \frac{v_0}{\sqrt{\left(\frac{\mu U_0}{2\rho L}\right)}}, \tag{10}$$

$$K_p = \frac{K_p^* U}{2\rho L},\ \mathrm{Re} = \frac{UL}{\upsilon},\ Ec = \frac{U^2 k}{C_p q_w}\sqrt{\frac{\mathrm{Re}}{2L^2}},\ Sc = \frac{\upsilon}{D},\ \beta = \frac{2LK_1}{U},\ J = Ec\,M$$

and writing the internal heat generation or observation q''' as (Chamkha and Khalend [24])

$$q''' = k\left(\frac{\mathrm{Re}}{2L^2}\right)\left[a^*(T_w-T_\infty)e^{-\eta}+b^*(T-T_\infty)\right] \tag{11}$$

Substituting (9), (10) and (11) in (2) – (4), we get $f'''+(1+\lambda_1)ff''-2(1+\lambda_1)f'^2-(1+\lambda_1)\left(M+\frac{1}{K_p}\right)f' = 0$

(12)

$$(1+R)\theta''+\mathrm{Pr}(\theta f'+\theta' f)+a^*e^{-\eta}+b^*\theta+Ec\,\mathrm{Pr}\,f''^2+J\,\mathrm{Pr}\,f'^2 = 0 \tag{13}$$

$$\phi''+Sc(\phi f'+f\phi')-Sc\beta\phi = 0 \tag{14}$$

The transformed boundary conditions are

$$f = f_w,\ f' = 1,\ \theta' = -1,\ \phi' = -1 \text{ at } \eta = 0 \tag{15}$$

$$f' \to 0,\ \theta \to 0,\ \phi \to 0 \text{ as } \eta \to \infty \tag{16}$$

In order to demonstrate the physical impact of non-dimensional factors, the linked nonlinear boundary value problems (12) - (14) were numerically solved using MATLAB BVP4c programming. The local skin-friction coefficient, the local Nusselt number, and the local Sherwood number are $f''(0)$, $-\theta'(0)$, and $-\phi'(0)$ all calculated and their numerical values are shown in a table.

3. Results and Discussion

Numerous factors, such as Jeffrey parameter λ_1, magnetic parameter M, porosity Kp and suction f_w and Prandtl number Pr and radiation R and heat production or absorption parameters $a*$ and $b*$ were computed numerically using the approach stated in the preceding paragraph. Eckert Ec and Schmidt numbers Sc were also employed. Dimensionless parameters λ_1, M, Kp and f_w the velocity field are shown in Figs. 2–5. Figure 2 depicts the impact on that is shown by λ_1

JOURNAL OF ALGEBRAIC STATISTICS
Volume 13, No. 2, 2022, p. 2619 - 2631
https://publishoa.com
ISSN: 1309-3452

on $f'(\eta)$. The flow is observed to be slowed as the concentration increases λ_1. The reduction in velocity is caused by an increase in drag forces. There is a consistent pattern in both cases of suction and injection. Voltage profile is shown in Fig. 3 as a function of the magnetic parameter. The conducting fluid creates a drag-like force known as Lorentz force, which reduces the fluid's speed. The same pattern may be seen in both suction ($f_w > 0$) and injection ($f_w < 0$). The velocity decreases as a result of the main directional flow being acted upon by the resistive force. It is easy to see the significant increase in velocity even in a low-intensity magnetic field. In order to regulate the flow of fluid in a clinical or mechanical situation, one may adjust the intensity of the external magnetic field. In Fig. 4 the porosity parameter Kp acts as helpful force for the fluid velocity i.e. the increasing values of Kp raises the velocity for suction as well as for injection. After a closer look, it is found that the rate of increase Kp slows significantly after the first 0.1 increments.

Figure 5 shows that when the suction parameter f_w is increased, the velocity decreases. So suction may be used to regulate the flow.

On the boundary layer fluid temperature profiles, as shown in Figures 6–13, the influence of dimensionless factors λ_1, M, Kp, f_w, $\Pr$, R, a^*, b^* and Ec can be clearly seen. Images 6–8 show how Jeffrey parameter λ_1, magnetic parameter M , and porosity parameters Kp affect the temperature profile of an object. As the Jeffrey λ_1 and Magnetic M parameters increase, we see an increase in temperature. Consider the fact that the temperature Kp is inversely proportional to the magnetic parameter. Lowering the temperature Kp is made possible by raising the value of yields. Suction parameter f_w affects temperature distribution in Fig. 9. The temperature lowers fast as the value of decreases f_w. Figure 10 depicts the relationship between temperature and the Prandtl number $\Pr$. Temperatures decline as a consequence of an increase in $\Pr$. It is known as the Prandtl number because it is the ratio of momentum to thermal diffusivity. To put it another way, the lower $\Pr$ the value of a certain fluid, the more dense $\Pr$ the gas it correlates to. As a result, a rise in $\Pr$ causes a sharp drop in temperature. According to the graph in figure 11, increasing the radiation parameter R causes a significant rise in temperature. Allows heat to be dissipated from the flow zone and cool the system by thickening the thermal barrier. Heat production and absorption characteristics a^*, b^* are shown in Fig. 12 as a function of the temperature profile. The findings show that the temperature drops as the absorption parameter $a^* < 0$ and $b^* < 0$ absorbs the heat from the sheet. Furthermore, $a^* > 0$ and $b^* > 0$ it is evident that the fluid's temperature rises in direct proportion to changes in the heat production or absorption characteristics a^* and b^*. Eckert number. as seen in Fig. 13. Improved Eckert number Ec increases kinetic energy since it is derived from the kinetic energy of flow and the difference in heat enthalpy. Again, it is well-known that the average kinetic energy of an object is determined by its temperature. Heat dissipation becomes more viscous, and the temperature rises. Due to the rise in temperature, the fluid Ec will become more viscous. Graphs show that as the temperature rises, so does the fluid. Increases in Ec and M result in a rise in the Joule Heating Parameter $J = Ec\,M$, which is defined as. Higher Joule heating parameter values may be explained by the fact that greater Eckert number and magnetic parameter assist boost temperature.

Dimensionless concentration behaviour for different material properties λ_1, M, Kp, f_w, β and Sc is shown in Figs. 14–19. As illustrated in Figs. 14 and 15, the fluid concentration rises as Jeffrey λ_1 and the magnetic M parameters are increased. The concentration of the fluid drops with increase of porosity parameter Kp and suction parameter f_w , which are clear from Figs.16 and 17. The influence of the reaction rate parameter β and the Schmidt number Sc on the concentration profile is seen in Figs. 18 and 19. The fluid's concentration increases β and Sc falls at the same time.

According to prior studies, the skin-friction coefficient $f''(0)$ for $Kp \to \infty$, $Ec = 0$, $\lambda_1 = 0$ values of Khadijah [25] and Swain et al. [26] were compared in Table 1 and determined to be in good agreement. Using various values of the Jeffrey

JOURNAL OF ALGEBRAIC STATISTICS
Volume 13, No. 2, 2022, p. 2619 - 2631
https://publishoa.com
ISSN: 1309-3452

parameter λ_1, magnetic parameter M, porosity parameter Kp, suction f_w, Prandtl number $\Pr$, radiation R and heat generation or absorption parameters $a*$ and $b*$ Eckert number Ec, reaction rate β, Schmidt number Sc and Eckert number, the values of skin friction coefficient, Nusselt number and Sherwood are shown in Table 2. When λ_1 and M are increased in value, it has been shown that the Sherwood number, skin friction coefficient, and Nusselt number all drop. With respect to the skin friction coefficient, Nusselt number, and Sherwood number, the porosity Kp and suction parameters f_w behave in the opposite way. There is a rise in $\Pr$, Ec, $a*$ and $b*$ the Nusselt number, whereas the trend in the opposite direction is found for R. The Sherwood number is thought to grow with an increase in Sc and β.

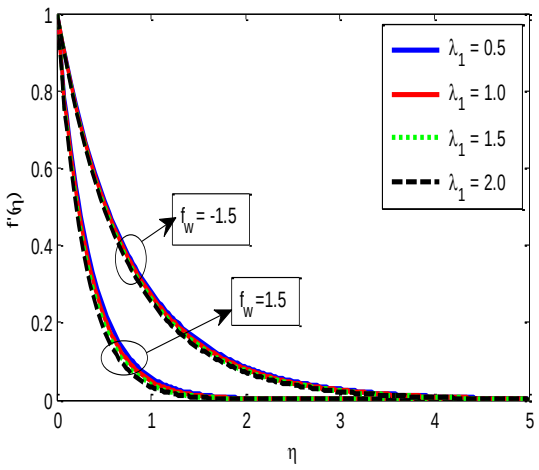

Fig. 2. Effects of Jeffrey parameter on velocity profile when $M=1, Pr=1, Ec=0.02, R=0.5, \beta=0.5, Kp=1, Sc=0.9, a*=0.2, b*=0.2$.

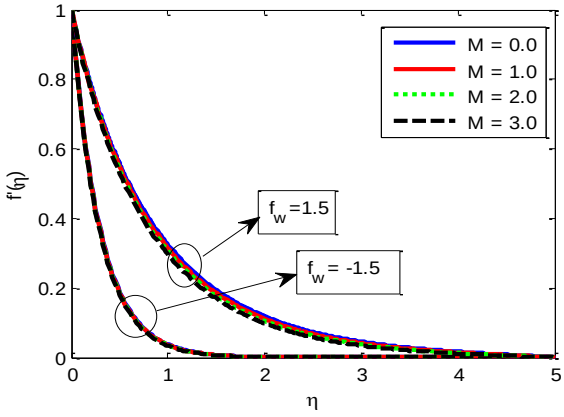

Fig. 3. Effects of magnetic parameter on velocity profile when $\lambda_1=0.5, Pr=1, Ec=0.02, R=0.5, \beta=0.5, Kp=1, Sc=0.9, a*=0.2, b*=0.2$.

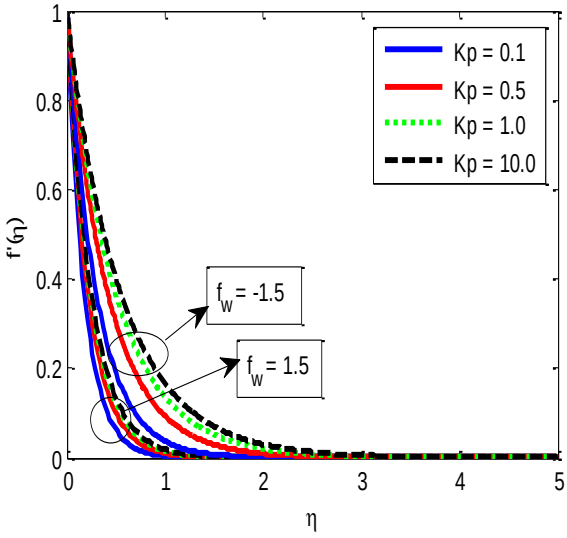

Fig. 4. Effects of porosity parameter on velocity profile when $\lambda_1=0.5, Pr=1, Ec=0.02, R=0.5, \beta=0.5, Kp=1, Sc=0.9, a*=0.2, b*=0.2, M=1$.

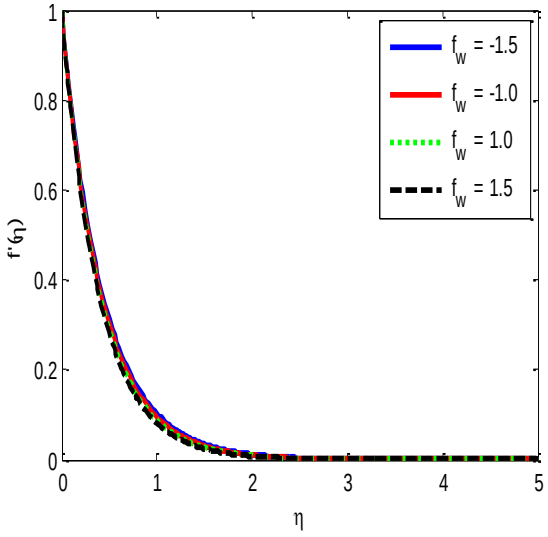

Fig. 5. Effects of suction parameter on velocity profile when $\lambda_1=0.5, Pr=1, Ec=0.02, R=0.5, \beta=0.5, Kp=1, Sc=0.9, a*=0.2, b*=0.2, M=1$.

JOURNAL OF ALGEBRAIC STATISTICS
Volume 13, No. 2, 2022, p. 2619 - 2631
https://publishoa.com
ISSN: 1309-3452

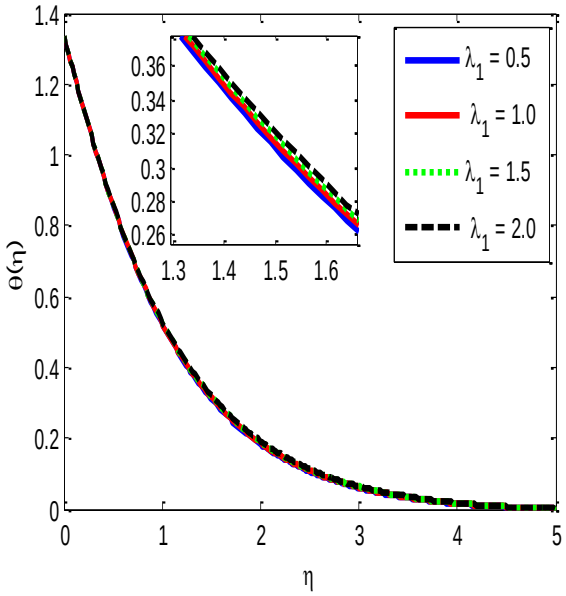

Fig. 6. Effects of Jeffrey parameter on temperature profile when $Pr = 1, Ec = 0.02, R = 0.5, \beta = 0.5, Kp = 1,$ $Sc = 0.9, a^* = 0.2, b^* = 0.2, M = 1, f_w = 1.5$.

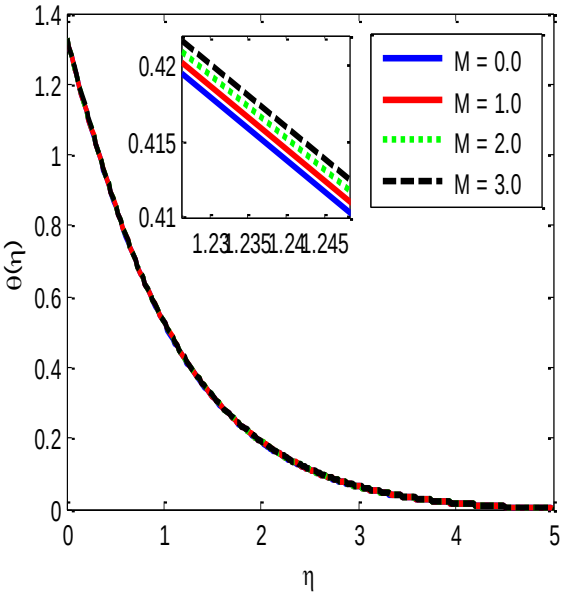

Fig. 7. Effects of magnetic parameter on temperature profile when $Pr = 1, Ec = 0.02, R = 0.5, \beta = 0.5, Kp = 1,$ $Sc = 0.9, a^* = 0.2, b^* = 0.2, \lambda_1 = 0.5, f_w = 1.5$.

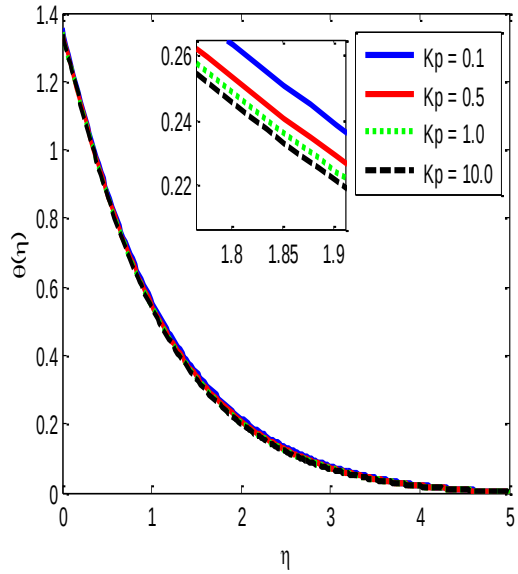

Fig. 8. Effects of porosity parameter on temperature profile when $Pr = 1, Ec = 0.02, R = 0.5, \beta = 0.5, \lambda_1 = 0.5,$ $Sc = 0.9, a^* = 0.2, b^* = 0.2, M = 1, f_w = 1.5$.

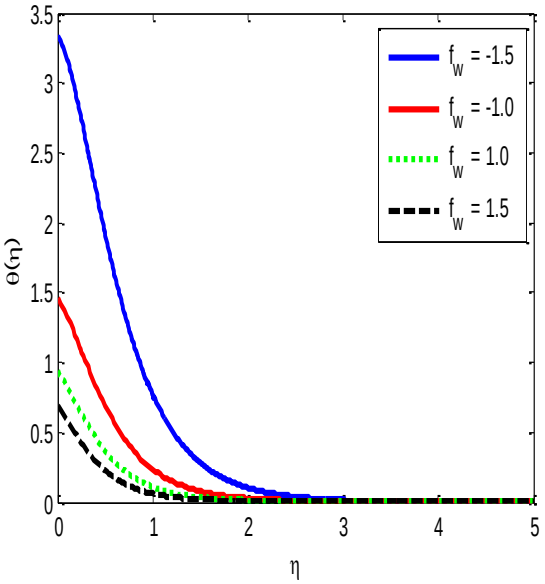

Fig. 9. Effects of suction parameter on temperature profile when $Pr = 7, Ec = 0.02, R = 0.5, \beta = 0.5, \lambda_1 = 1,$ $Sc = 0.9, a^* = 0.2, b^* = 0.2, M = 1, Kp = 1$.

JOURNAL OF ALGEBRAIC STATISTICS
Volume 13, No. 2, 2022, p. 2619 - 2631
https://publishoa.com
ISSN: 1309-3452

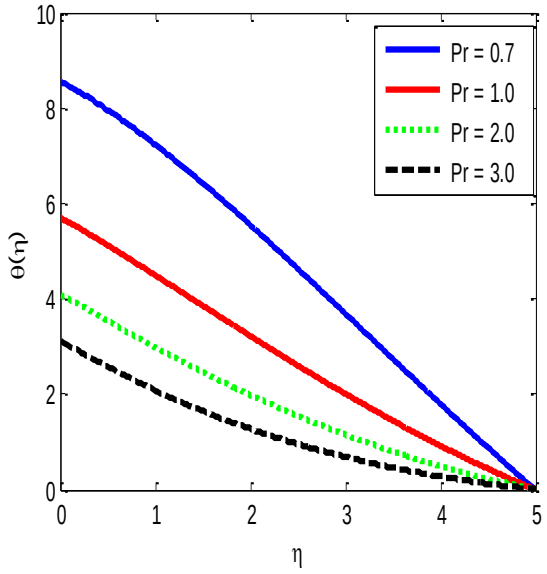

Fig. 10. Effects of Prandtl number on temperature profile when $Sc = 0.9, Ec = 0.02, R = 0.5, \beta = 0.5, \lambda_1 = 1, M = 2,$ $f_w = 1.5, a^* = 0.1, b^* = 0.1, Kp = 1$.

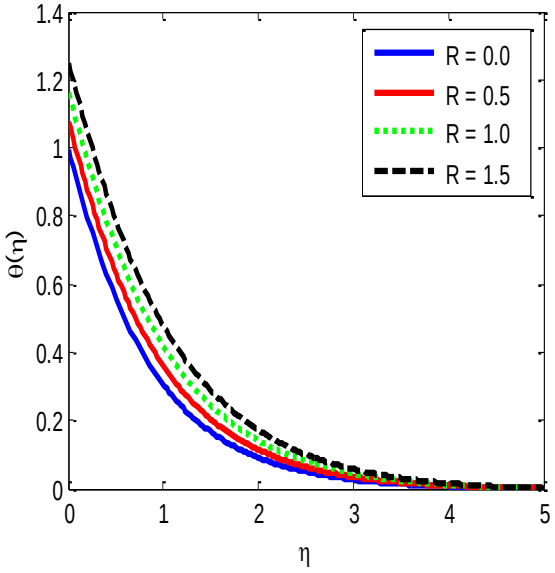

Fig. 11. Effects of radiation parameter on temperature profile when $Sc = 0.9, Ec = 0.02, \Pr = 1, \beta = 0.5, \lambda_1 = 1,$ $f_w = 1.5, a^* = 0.2, b^* = 0.2, M = 1, Kp = 1$.

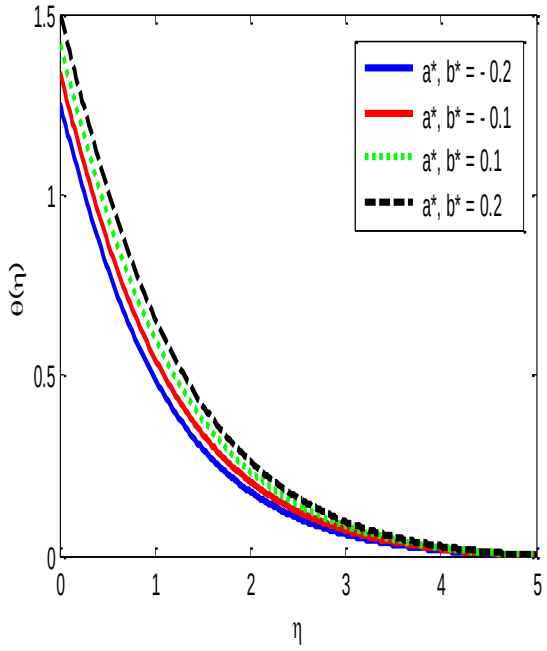

Fig. 12. Effects of heat generation or absorption parameters on temperature profile when $Sc = 0.9,$ $Ec = 0.02, \Pr = 1, \beta = 0.5, \lambda_1 = 1, f_w = 1.5, M = 1, Kp = 1$.

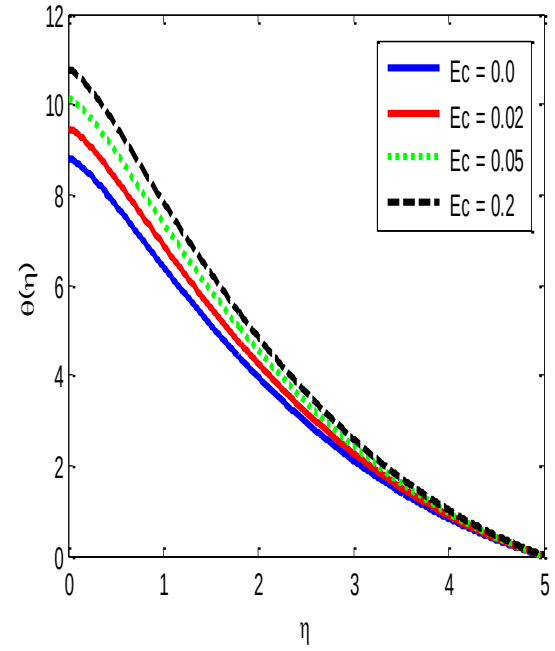

Fig. 13. Effects of Eckert number on temperature profile when $Sc = 0.9, \Pr = 1, \beta = 0.5, \lambda_1 = 1, f_w = 0.5, a^* = 0.2,$ $b^* = 0.2, M = 1, Kp = 1$.

JOURNAL OF ALGEBRAIC STATISTICS
Volume 13, No. 2, 2022, p. 2619 - 2631
https://publishoa.com
ISSN: 1309-3452

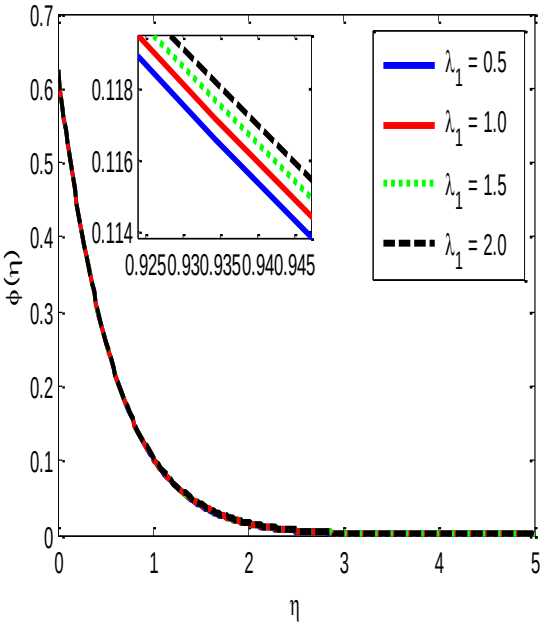

Fig. 14. Effects of Jeffrey parameter on concentration profile when $Sc = 0.9, \Pr = 1, \beta = 0.5, f_w = 1.5, a^* = 0.2, b^* = 0.2, M = 1, Kp = 1$.

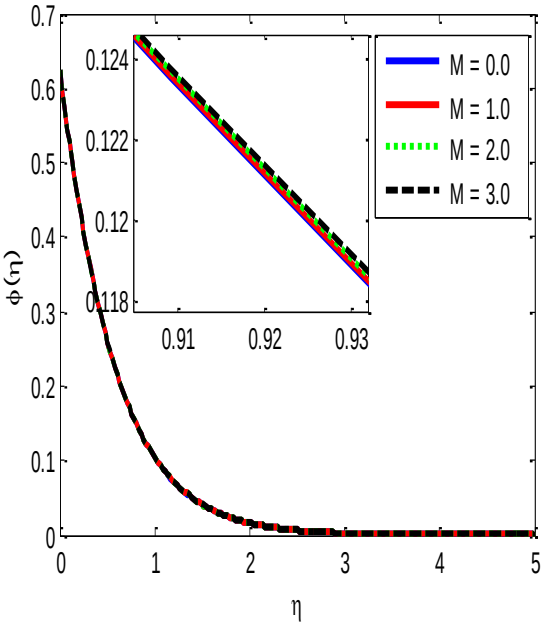

Fig. 15. Effects of magnetic parameter on concentration profile when $Sc = 0.9, \Pr = 1, \beta = 0.5, f_w = 1.5, a^* = 0.2, b^* = 0.2, \lambda_1 = 0.5, Kp = 1$.

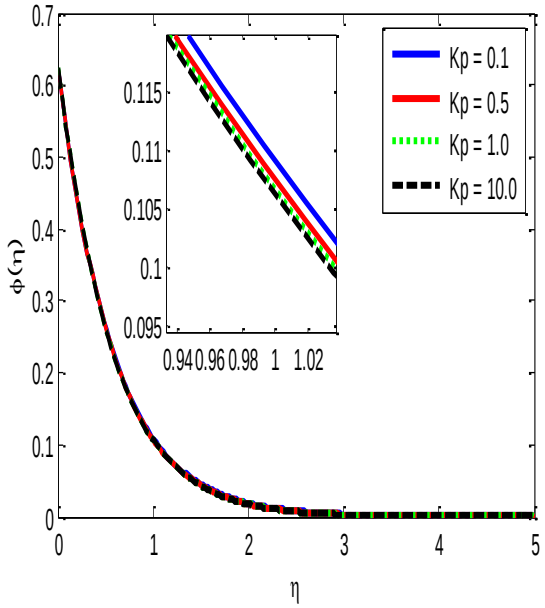

Fig. 16. Effects of porosity parameter on concentration profile when $Sc = 0.9, \Pr = 1, \beta = 0.5, f_w = 1.5, a^* = 0.2, b^* = 0.2, M = 1, \lambda_1 = 0.5$.

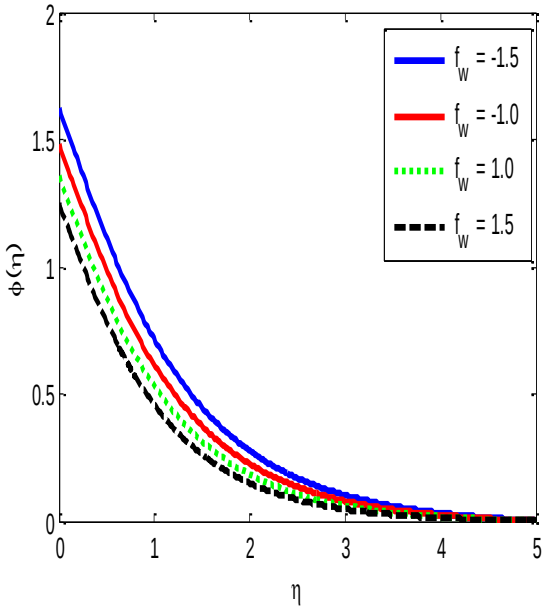

Fig. 17. Effects of suction parameter on concentration profile when $Sc = 0.9, \Pr = 1, \beta = 0.5, \lambda_1 = 0.5, a^* = 0.2, b^* = 0.2, M = 1, Kp = 1$.

JOURNAL OF ALGEBRAIC STATISTICS
Volume 13, No. 2, 2022, p. 2619 - 2631
https://publishoa.com
ISSN: 1309-3452

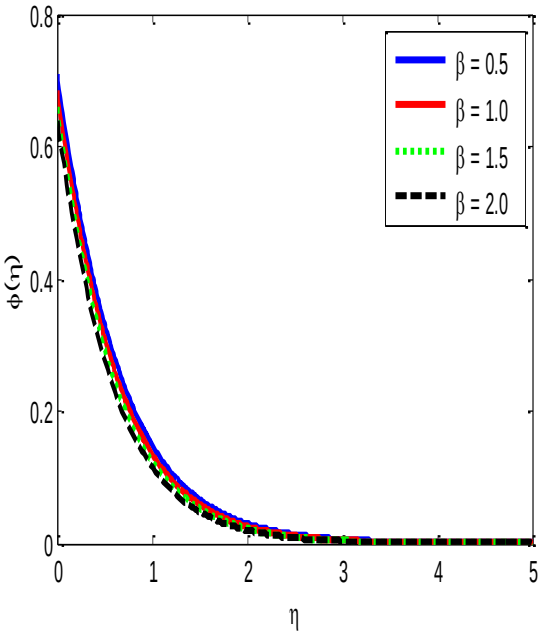

Fig. 18. Effects of reaction rate parameter on concentration profile when $Sc = 0.9, \Pr = 1, \lambda_1 = 1,$ $f_w = 1.5, a^* = 0.2, b^* = 0.2, M = 1, Kp = 1$.

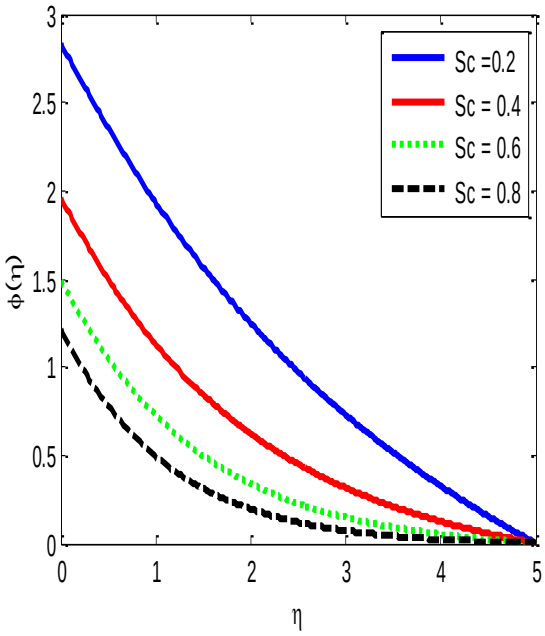

Fig. 19. Effects of Schmidt number on concentration profile when $\lambda_1 = 1, \Pr = 1, \beta = 0.5, f_w = 1.5, a^* = 0.2,$ $b^* = 0.2, M = 1, Kp = 1$.

Table 1: Validation of the present values of $f''(0)$ when $R = 0.5, \Pr = 1, \lambda_1 = 0, a^* = 0.2,$ $b^* = 0.2, Kp \to \infty, Ec = 0, \lambda_1 = 0$.

	Khadijah [25]	**B.K. Swain et al. [26]**	**Present study**
$M = 0$	-2. 20348	-2.203913	-2.204012
$M = 1.5$	-2.65822	-2.658565	-2.659324
$f_w = 1$	-2.02809	-2.028286	-2.028342
$f_w = 2$	-2.74565	-2.745943	-2.746104

JOURNAL OF ALGEBRAIC STATISTICS
Volume 13, No. 2, 2022, p. 2619 - 2631
https://publishoa.com
ISSN: 1309-3452

Table 2: The values of skin friction coefficient, Nusselt number and Sherwood number for various values of

λ_1	Kp	M	R	Pr	a^*	b^*	Ec	Sc	β	f_w	$f''(0)$	$-\theta'(0)$	$-\phi'(0)$
0.5											-1.424355	1.857161	1.684280
1.0											-1.531996	1.852756	1.682379
1.5											-1.622307	1.849306	1.680654
	0.1										-3.667566	1.789631	1.630006
	0.5										-1.827704	1.841422	1.673434
	1.0										-1.531996	1.852756	1.682379
		0.5									-1.375458	1.857375	1.687349
		1.0									-1.531996	1.852756	1.682379
		1.5									-1.682576	1.848437	1.677752
			0.5								-1.375458	1.857375	1.687349
			1.0								-1.375458	1.627524	1.687349
			1.5								-1.375458	1.494508	1.687349
				0.7							-1.375458	1.584792	1.687349
				1.0							-1.375458	1.857375	1.687349
				2.0							-1.375458	2.836389	1.687349
					-0.1	-0.1					-1.375458	1.835060	1.687349
					0.0	0.0					-1.375458	1.842323	1.687349
					0.3	0.3					-1.375458	1.864740	1.687349
							0.0				-1.375458	1.850389	1.687349
							0.02				-1.375458	1.857375	1.687349
							0.03				-1.375458	1.860868	1.687349
								0.2			-1.375458	1.857375	1.265251
								0.4			-1.375458	1.857375	1.543798
								0.6			-1.375458	1.857375	1.833381
									0.3		-1.375458	1.857375	1.657488
									0.5		-1.375458	1.857375	1.687349
									0.7		-1.375458	1.857375	1.716863
										1.0	-1.612907	1.630396	1.527847
										1.5	-1.375458	1.857375	1.687349
										2.0	-1.190462	2.097674	1.854325

λ_1, Kp, M, R, Pr, a^*, b^*, Ec, Sc, β, f_w.

4. Conclusion

Jeffrey fluid flow with viscous dissipation through porous stretched sheet is explored in the current inquiry for the influence of chemical reaction on MHD heat and mass transfer. As a result, we may draw the following conclusions.

- Velocity profile enhances for porosity parameter and decrease for the Jeffrey parameter and magnetic parameter.
- Temperature profile found to increases Jeffrey parameter and magnetic parameter. Decreases for the Prandtl number.
- Heat generation/absorption parameters that have positive values tend to cool things down, while those that have negative values do the opposite.
- Increasing the temperature distribution requires an increase in the Eckert number. As a result of dissipation, the energy accumulates in the fluid zone. In order to increase the thickness of the thermal boundary layer, the radiation parameter is used.
- Concentration profiles were found to increase for Jeffrey parameter and magnetic parameter. Decreases for porosity parameter, reaction rate parameter and Schmidt number.

References

[1] Kothandapani, M. and Srinivas, S. (2008) Peristaltic transport of a Jeffrey fluid under the effect of magnetic field in an asymmetric channel. Int. J. Non-Lin. Mech., 43, 915 –924.

[2] Tripathi, D., Ali, N., Hayat, T., Chaube, M.K., Hendi, A.A.(2011) Peristaltic flow of MHD Jeffrey fluid through a finite length cylindrical tube. Appl. Math. Mech. Engl. Edit., 32, 1148 –1160.

[3] Hayat, T., Awais, M. and Alsaedi, A. (2012) Newtonian heating and Magnetohydrodynamic effects in flow of a Jeffrey fluid over a radially stretching. Int. J. Physical Sci., 7, 2838–2844.

[4] Abbasi, F.M., Shehzad, S.A., Hayat, T., Alsaedi, A. and Obid, M.A. (2015) Influence of heat and mass flux conditions in hydromagnetic flow of Jeffrey nanofluid. AIP Advances, 5, 037111.

[5] Farooq, M., Gull, N., Hayat, T. and Alsaedi, A. (2015) MHD flow of Jeffrey fluid with Newtonian heating. J. Mech., 1–11, doi: 10.1017/jmech.2014.93.

[6] Sudheer Babu, M., Reddappa, B. and S. Sreenadh, S. (2022) Effect of second order chemical reaction and double stratification on MHD free convection flow of Casson fluid over an exponentially stretching sheet through porous medium. Gorteria Journal, 35(3), 53-66.

[7] Abo-Eldahab, E.M. and Salem, A.M. (2004) Hall Effect on MHD Free Convection Flow of a Non-Newtonian Power Law Fluid at a Stretching Surface. International Communications in Heat and Mass Transfer, 31, 343-354. http://dx.doi.org/10.1016/j.icheatmasstransfer.2004.02.005

[8] Chakrabarti, A. and Gupta, A.S. (1979) Hydromagnetic Flow and Heat Transfer over a Stretching Sheet. Quarterly of Applied Mathematics, 37, 73-78.

[9] Vajravelu, K. and Hadjinicolaou, A. (1993) Heat Transfer in a Viscous Fluid over a Stretching Sheet with Viscous Dissipation and Internal Heat Generation. International Communications in Heat and Mass Transfer, 20, 417-430. http://dx.doi.org/10.1016/0735-1933(93)90026-R.

[10] Chamkha, A.J., Mujtaba, M., Quadri, A. and Issa, C. (2003) Thermal Radiation Effects on MHD Forced Convection Flow Adjacent to a Non-Isothermal Wedge in the Presence of a Heat Source or Sink. Heat and Mass Transfer, 39, 305-312.

[11] Abo-Eldahab, E.M. and El Aziz, M.A. (2005) Viscous Dissipation and Joule Heating Effects on MHD-Free Convection from a Vertical Plate with Power-Law Variation in Surface Temperature in The presence of Hall and Ion-Slip Currents. Applied Mathematical Modeling, 29, 579-595. http://dx.doi.org/10.1016/j.apm.2004.10.005.

[12] Jaber, K.K. (2012) Transient MHD Mixed Double Diffusive Convection along a Vertical plate Embedded in a Non-Darcy Porous Medium with Suction or Injection. Journal of Mathematics and Statistics, 8, 1.

[13] Aboeldahab, E.M. and Elbarbary, E.M.E. (2001) Hall Current Effect on Magnetohydrodynamic Free-Convection Flow past a Semiinfinite Vertical Plate with Mass Transfer. International Journal of Engineering Science, 39, 1641-1652. http://dx.doi.org/10.1016/S0020-7225(01)00020-9.

[14] Abo-Eldahab, E.M. and Mohamed, A.E. (2004) Hall Current and Ohmic Heating Effects on Mixed Convection Boundary Layer Flow of a Micropolar Fluid from a Rotating Cone with Power-Law Variation in Surface Temperature. International Communications in Heat and Mass Transfer, 31, 751-762.

[15] Jaber, K.K. (2014) Effect of Hall Currents and Variable Fluid Properties on MHD Flow past Stretching Vertical Plate by the Presence of Radiation. Journal of Applied Mathematics and Physics, 2, 888-902.

[16] Jaber, K.K. (2014) Effect of Viscous Dissipation and Joule Heating on MHD Flow of a Fluid with Variable Properties past a Stretching Vertical Plate. European Scientific Journal, 10.

[17] Mandal, G. and Mandal, K.K. (1983) Effect of Hall Current on MHD Couette Flow between Thick Arbitrarily Conducting Plates in a Rotating System. Journal of the Physical Society of Japan, 52, 470-477. http://dx.doi.org/10.1143/JPSJ.52.470

[18] Mandal, I.C. and Mukhopadhyay, S. (2013) Heat Transfer Analysis for Fluid Flow over an Exponentially Stretching Porous Sheet with Surface Heat Flux in Porous Medium. Ain Shams Engineering Journal, 4, 103-110. http://dx.doi.org/10.1016/j.asej.2012.06.004

[19] Reddappa, B. and Sreenadh, S. (2022) Double stratification effects on electrical MHD free convection Jeffrey flow of second order chemical reactions over an exponentially stretching sheet. Adalya Journal, 11(4), 21-35. https://doi.org/10.37896/aj11.4/003.

[20] Reddappa, B., Parandhama, A., Venkateswara Raju, K. and Sreenadh, S. (2021) Analysis of the boundary layer flow of thermally conducting Jeffrey fluid over a stratified exponentially stretching sheet. Turkish Journal of Computer and Mathematics Education, Vol.12 No.13 (2021), 730-739.

[21] Nagur Meeraiah, P., Reddappa, B. and Saila Kumari, A. (2020) Unsteady MHD boundary layer flow and heat transfer of a Casson fluid past a stretching sheet. International Journal of Mechanical and Production Engineering Research and Development, 10(3), 12365-12374.

[22] Hossain, M. A., Alim, M. A. and Rees, D. A. S. (1998) The effect of radiation on free convection from a porous vertical plate. International Journal of Heat and Mass Transfer, 42 (1), 181 –191.

[23] Raptis, A. (1998) Flow of a micropolar fluid past a continuously moving plate by the presence of radiation. Int. J. Heat Mass Tran. 41, 2865 –2866.

[24] Chamkha, A.J. and Khaled, A.A. (2001) Similarity solutions for hydromagnetic simultaneous heat and mass transfer by natural convection from an inclined plate with internal heat generation or absorption. Heat Mass Tran. 37, 117–123.

[25] Kadijah, M.A. (2018) Numerical studies for MHD flow and gradient heat transport past a stretching sheet with radiation and heat production via DTM. Appl. Appl. Math, 13, 915 – 924.

[26] Swain, K., Parida, B.C., Kar, S. and Senapati, N. (2020) Viscous dissipation and joule heating effect on MHD flow and heat transfer past a stretching sheet embedded in a porous medium. Heliyon, 6, 1-8. https://doi.org/10.1016/j.heliyon.2020.e05338.